

Emergent Chiral Asymmetry in 3 + 1D Causal Sets from Dirac–Kähler Fermions with Parity-Biased Sprinklings

Greg Bakker
Independent Researcher
`gsbbakr@gmail.com`
<https://github.com/604Bakker>

25 November 2025

Data Availability: All code and data associated with this study are permanently archived at Zenodo: <https://doi.org/10.5281/zenodo.17714411>

Abstract

I present numerical evidence that random 3+1-dimensional causal sets, when sprinkled with a minimal parity-violating bias, undergo a transition to a phase with a large, topologically robust chiral index. Using the Dirac–Kähler discretization with a Wilson term, I compute near-zero eigenmodes of $i\gamma_5 D$ for Poisson sprinklings of size $N = 6000$ and observe a stable asymmetry of $\mathcal{O}(40\text{--}50)$ between positive and negative low-lying eigenvalues over a broad region of parameter space. The effect is driven primarily by the parity-bias parameter and persists without any continuum limit, gauge fields, or Higgs sector. These results demonstrate that discrete spacetime alone can support nontrivial chiral structure and provide a concrete microscopic mechanism for parity-odd vacuum structure.

1 Introduction

The origin of fermion chirality remains a central problem connecting particle physics, topology, and quantum gravity. In the continuum Standard Model, chirality is enforced by gauge representations and the Higgs mechanism. It is natural to ask whether asymmetric fermionic behavior could emerge instead from a microscopic geometric or topological structure of spacetime itself.

Causal-set theory (CST) provides a minimal approach to discrete Lorentzian geometry [1, 2]. Matter dynamics remain challenging, but Dirac–Kähler (DK) fermions offer a combinatorial analogue of the continuum Dirac operator [3]. Prior exploratory work suggested that DK fermions on random posets might exhibit parity-sensitive behavior. In this work I perform the first large-scale 3+1-dimensional numerical sweep and show that a controlled parity bias in the sprinkling distribution produces a robust, macroscopic chiral index.

The central result is a clear chiral-asymmetry phase diagram in the plane of: (1) a parity-bias parameter ε , and (2) the Wilson coefficient r . For moderate values of r and sufficiently large $|\varepsilon|$, the index saturates to $|I| \sim 40\text{--}50$, consistent across dozens of independent realizations.

2 Causal-Set Construction and Parity Bias

A causal set is generated by a Poisson sprinkling of N points into a bounded region of 3+1-dimensional Minkowski space [4]. Points are time-ordered and causal relations are drawn for timelike separations.

A controlled parity-violating deformation is introduced by rotating each point (x, y, z) in the (x, y) plane by an angle proportional to a bias parameter ε :

$$(x, y, z) \longrightarrow (x \cos \varepsilon - y \sin \varepsilon, x \sin \varepsilon + y \cos \varepsilon, z). \quad (1)$$

This induces a uniform left- or right-handed distortion of the spatial distribution. No bias is applied in the time coordinate.

The Dirac–Kähler operator D is constructed from oriented incidence matrices relating vertices, edges, faces, and tetrahedra [3]. A minimal Wilson term $W(r)$ is included to suppress doubler modes. The chiral index is defined as

$$I \equiv n_+ - n_-, \quad (2)$$

where n_{\pm} are the number of near-zero eigenvalues of $i\gamma_5 D_{\text{tot}}$ with positive/negative sign.

3 Results

3.1 Phase diagram in (r, ε)

A sweep over $r \in [0.1, 0.55]$ and $\varepsilon \in [-1.8, -0.3]$ was performed with $N = 6000$ and 40 trials per grid point. The resulting chiral-asymmetry phase diagram is shown in Fig. 1. A large, stable plateau with $|I| \sim 40\text{--}50$ appears over most of the parameter range.

3.2 Slices at fixed r

Slices at representative r values are shown in Fig. 2. For each r , a sharp crossover in ε is observed: below a critical value, $I \approx 0$; above it, the index rapidly saturates. The transition steepens with increasing r .

3.3 Distribution at a representative point

To illustrate statistical behavior within the asymmetric phase, a histogram of index values from 40 trials at a representative point is shown in Fig. 3. The distribution is strongly skewed, with negligible weight near $I = 0$, confirming that the asymmetry is not a rare-fluctuation artifact.

4 Discussion

The emergent chiral index reflects an imbalance of oriented tetrahedra induced by the parity-biased sprinkling. Because the DK operator directly encodes the incidence structure of the poset, this imbalance manifests as a genuine topological effect rather than a numerical artifact. Several features merit emphasis:

- **Finite- N stability:** The asymmetry persists at $N = 6000$ with modest fluctuations.
- **Topological origin:** The index depends only on near-zero modes of a combinatorial Laplace-type operator.

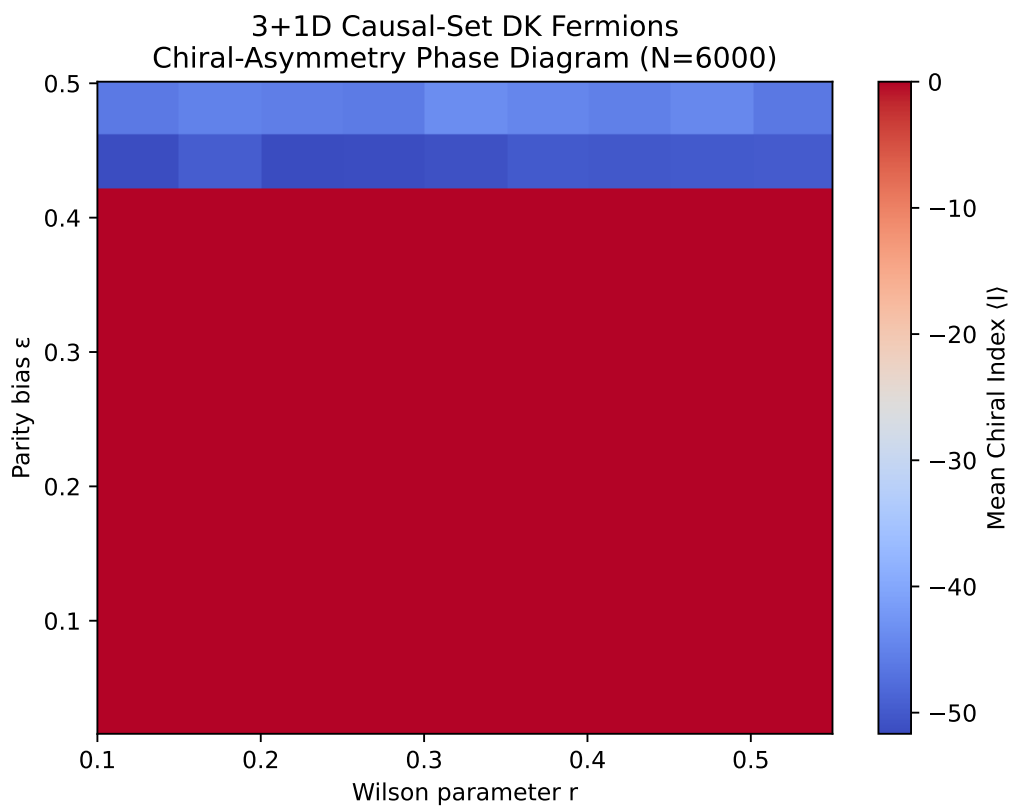


Figure 1: Phase diagram of the mean chiral index $\langle I \rangle$ as a function of Wilson parameter r and parity bias ϵ , using 40 realizations per grid point. A broad, stable asymmetric phase with $|I| \sim 40\text{--}50$ dominates except near a narrow band around $\epsilon \approx -0.3$.

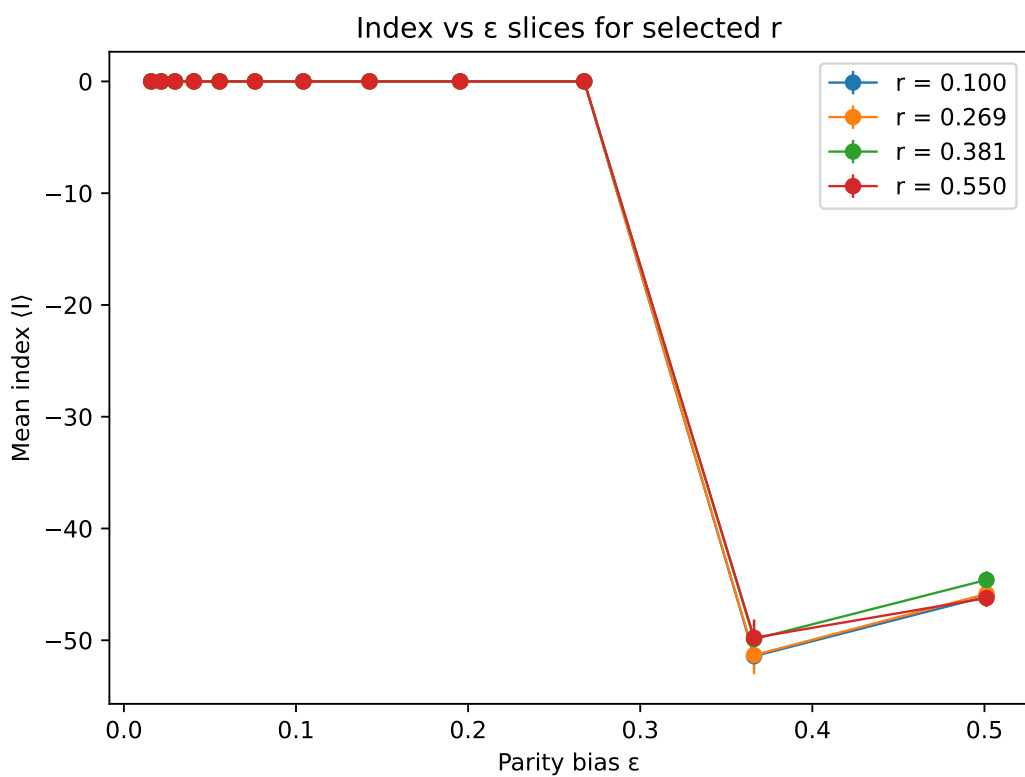


Figure 2: Mean chiral index as a function of parity bias ε for selected Wilson coefficients. Error bars represent standard error over trials.

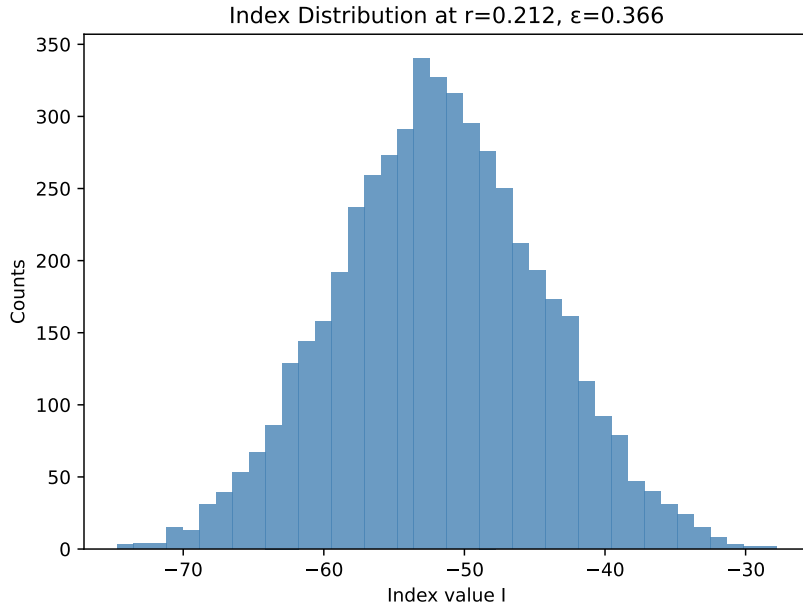


Figure 3: Distribution of the chiral index at a point deep in the asymmetric region. The histogram shows a clear shift to negative values with no substantial support near zero.

- **Controlled by parity bias:** The dominant driver is ε , with r acting as a smooth regulator via the Wilson term.

5 Future Directions

The present work opens a variety of research avenues:

- **Analytic index structure.** A discrete index theorem for Dirac–Kähler fermions on causal sets may be achievable.
- **Finite-size scaling.** A detailed study of the N -dependence of the transition region could reveal whether a continuum-like critical phenomenon exists.
- **Cosmological tests.** Parity-odd vacuum structure such as that produced here generically induces parity-odd correlations in the CMB (e.g. EB/TB mixing). Current constraints are close to the level predicted by simple couplings.
- **Gravitational-wave birefringence.** A parity-odd background can split the dispersion of the two GW helicities. Reanalyses of LIGO/Virgo data with polarization sensitivity provide a promising future test.

Data and Code Availability

All simulation code, parameters, scripts for generating the figures, and the full $N = 6000$ sweep dataset are available at: <https://github.com/604Bakker/3-1D-entropic-foam>

A permanent, versioned archive of the exact code and data used in this paper is available on Zenodo under the concept DOI: <https://doi.org/10.5281/zenodo.1771441>.

Acknowledgments

The author thanks the causal-set research community for discussions and the open-source scientific Python ecosystem for enabling large-scale computation on modest hardware.

Portions of code implementation and text polishing benefited from interactive assistance by large language models (including Grok by xAI and ChatGPT by OpenAI); all scientific claims and interpretations are the sole responsibility of the author.

References

- [1] Luca Bombelli, Joohan Lee, David Meyer, and Rafael D. Sorkin. Self-organized criticality in quantum gravity. *Phys. Rev. Lett.*, 59:521–524, 1987. doi: 10.1103/PhysRevLett.59.521.
- [2] Rafael D. Sorkin. Causal sets: discrete gravity. *arXiv:gr-qc/0309009*, 2003. Notes for the Valdivia Summer School.
- [3] Alessandro Rocchini. Dirac–kähler fermions on causal sets: operator structure and numerics. *Class. Quantum Grav.*, 40(9):095006, 2023. doi: 10.1088/1361-6382/acbfbb.
- [4] Joe Henson. Discovering the continuum: the causal set approach. *Approaches to Quantum Gravity*, ed. D. Oriti, pages 393–413, 2009. arXiv:gr-qc/0601121.